

Investigations Concerning the Coupled Wing-Fuselage-Tail Flutter Phenomenon

W. J. MYKYTOW,* T. E. NOLL,† L. J. HUTTSELL,† AND M. H. SHIRK‡
Air Force Flight Dynamics Laboratory, Wright-Patterson Air Force Base, Ohio

Results of subsonic model tests and analyses of a critical mode of flutter of a wing-fuselage-horizontal tail combination are presented. Increasing wing sweep can lead to lower flutter speeds. Flutter speeds are a minimum for cantilever wing bending to fuselage torsion frequency ratios in the range of 0.3–0.6. Vertical separation or dihedral angle increases the flutter speed and is more important than longitudinal separation. The aerodynamic interference effect of the wing on the tail is important and a detrimental feature for the configuration used. Flutter analyses using doublet lattice and kernel function unsteady aerodynamics methods were conducted to evaluate the accuracy of the prediction methods and to define controlling criteria. Also, experimental flutter model data and theoretical comparisons in the Mach number range of 0.6 to about 1.0 obtained in investigations conducted for the Air Force Flight Dynamics Laboratory are presented. In general, agreement between predicted and test results for subsonic and transonic investigations is good. Finally, aerodynamic prediction methods are applied to the wing-horizontal tail configuration selected by AGARD for comparisons.

Nomenclature

b	= reference semichord in streamwise direction, ft
b_o	= reference semichord measured streamwise and intersecting the elastic axis line 75% of the latter's length, ft
c	= local streamwise chord, ft
C_l	= local lift coefficient
C_m	= local moment coefficient
f	= frequency, Hz
m_i	= lumped mass at station i , slugs
M_∞	= freestream Mach number
Q_{ij}	= generalized force coefficient
s	= wing semispan, ft
$\bar{X}, \Delta X$	= wing-horizontal tail longitudinal separation, ft
$\bar{Z}, \Delta Z$	= vertical offset between wing and horizontal tail centerline, ft
V	= freestream velocity at flutter, fps
μ	= model to air mass ratio, $m/\pi\rho b^2$
ω	= flutter frequency, rad/sec
ω_h	= wing first cantilever bending frequency, rad/sec
ω_θ	= uncoupled fuselage torsion frequency, rad/sec

Introduction

SIGNIFICANT changes in the flowfield can be induced by lifting surfaces and/or bodies in close proximity. This interaction or interference can appreciably affect the angle of attack of the flow, and therefore the pressure or loading over the nearby lifting surface or body. These significant effects have long been demonstrated by both tests and theory in the static aerodynamics area. The aerodynamicist has in fact for some time used gross correction factors¹ in the form of mean downwash angles or employed more refined approaches using advances in aerodynamic theory.² On the other hand, the aeroelastician has been hampered in design flutter analyses because theoretical methods to predict unsteady aerodynamic loads for general cases involving interference have been lacking. Approximate corrections based on steady-state

measurements were therefore used in flutter analyses to account for the aerodynamic interference that occurs around a T-tail when such designs appeared about 1950. The criticality of the T-tail design from a flutter viewpoint spurred emphasis on the development of nonplanar theories to predict T-tail unsteady aerodynamic loads.^{3,4} A similar emphasis to predict unsteady aerodynamic loads for tandem surfaces, such as wing-horizontal tail combinations, was delayed until fairly recently since coupling of elastic modes to produce a critical flutter mode involving mechanical interaction of the wing, fuselage and tail was not encountered. Fortunately, a considerable theoretical foundation^{5–10} had been formulated in the early 1960's which facilitated the extension of unsteady load prediction methods to include wing-horizontal tail interaction. This body of information was rapidly expanded by further notable contributions.^{11–14} The first generation Albano-Rodden doublet lattice method,^{13,15} the second generation doublet lattice method¹⁶ and the Albano kernel function method,¹⁵ an extension of the Laschka kernel function method,¹¹ are of particular interest for the subsonic investigations reported herein.

The impetus for concentrated efforts in theoretical and further flutter model investigations of the coupled wing-fuselage-tail flutter problem was provided by Topp et al.¹⁷ in 1966. Figure 1 reproduces some of their subsonic flutter model test results for a fighter having a variable sweep wing. For low-wing sweep angles, the critical flutter modes are those mainly involving higher frequency bending and torsion motions of the lifting surfaces. For wing sweep angles above 58°, increasing the wing sweep angle produces a rapid drop in the flutter speed in a new flutter mode involving lower frequency modes of the wing, fuselage and tail. The proper trend of flutter speed could not be predicted¹⁷ until wing-tail unsteady aerodynamic interference was included.¹⁸ The

Received April 15, 1971; presented as Paper 71-326 at the AIAA/ASME 12th Structures, Structural Dynamics and Materials Conference, Anaheim, Calif., April 19–21, 1971; revision received August 20, 1971.

Index categories: Aeroelasticity and Hydroelasticity; Aircraft and Component Wind Tunnel Testing; and Aircraft Structural Design.

* Assistant for Research and Technology, Vehicle Dynamics Division. Associate Fellow AIAA.

† Aerospace Engineer. Associate Member AIAA

‡ Aerospace Engineer.

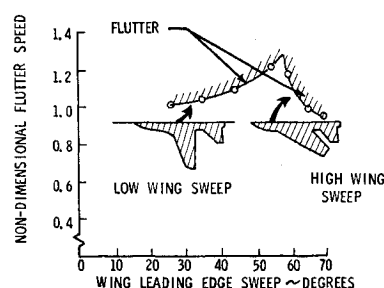


Fig. 1 Wing-fuselage-tail flutter.

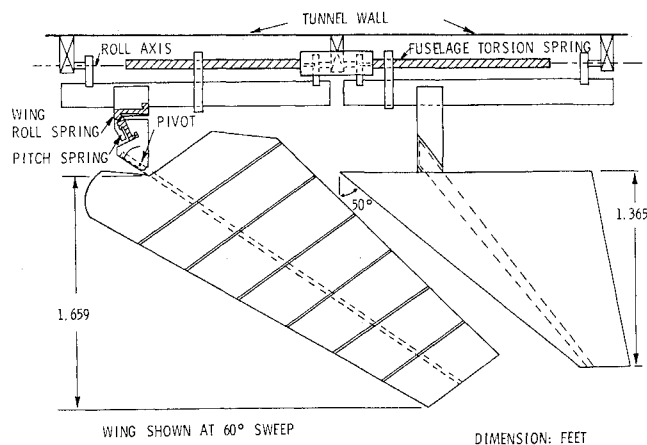


Fig. 2 Schematic of AFFDL subsonic wing-horizontal tail flutter model.

rapid and large drop in flutter speed inferred a potential criticality which stimulated rapid and excellent contributions in both theoretical and flutter model trend investigations.¹⁹⁻²²

AFFDL Flutter Model

The AFFDL flutter model²³ was a half-span simulation of a potential, variable-sweep-wing fighter. A schematic of the fuselage mechanism and suspension system is presented in Fig. 2. The model was tested in the Air Force Institute of Technology's 5 ft, subsonic, circular wind tunnel. The model wing stiffnesses were concentrated in a metal spar. The wing consists of seven separate balsa sections attached to the spar near the section centers. Typical fighter pivot roll and pitch stiffnesses were simulated near the wing root. A variable-length torsion bar arrangement was located within the fuselage fairing and permitted variation of the effective fuselage torsional stiffness and thus frequency. The stabilizer construction consisted of a metal spar covered with balsa wood. The stabilizer position could be varied horizontally and rotated to give 45° dihedral relative to the wing plane. Figure 3 illustrates the geometry variations possible with this model.

The wing, wing pivot support, fuselage torsion bar and horizontal tail flexibility coefficients were measured. In addition, weight, unbalance and inertia characteristics were also measured where possible. Natural modes and frequencies were computed using classic methods defined by Bisplinghoff et al.²⁴ and Dugundji.²⁵ Figure 4 shows typical results for the four elastic modes used in the flutter analyses. In general,

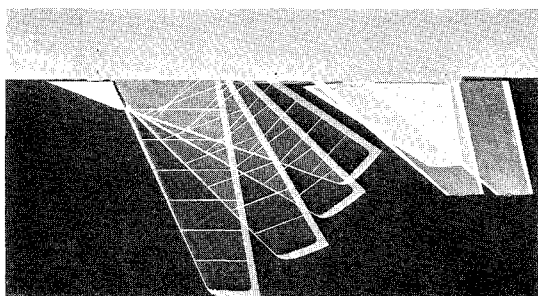


Fig. 3 AFFDL Wing-horizontal tail flutter model.

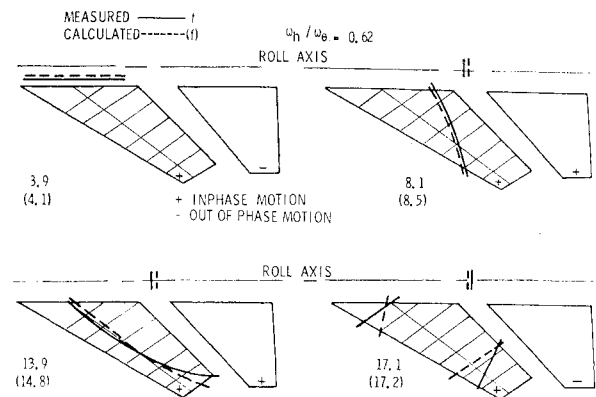


Fig. 4 Comparison of calculated and measured vibration node lines and frequencies.

agreement between measured and predicted modes and frequencies is excellent. The first two modes primarily involve coupling between wing bending and fuselage torsion. The third mode is primarily a wing carry-through pitch mode coupled with wing bending and fuselage torsion. The fourth mode is a second wing bending-fuselage torsion mode coupled with the pitch and wing torsion. Since the model was suspended from the ceiling by bearings, it was free to roll with gravity providing a roll frequency near 1.0 Hz.

Subsonic Flutter Model Results and Discussion

Several important variables were investigated during model wind-tunnel testing. Longitudinal wing-horizontal tail separation was varied over a range of practical values. The fuselage torsional frequency was also varied since it was expected that a mechanical tuning between wing modes and the fuselage torsion mode could lead to minimum flutter speeds at critical frequency ratios. Wing sweep was variable to simulate the range achievable in flight (25-70°, Fig. 3). Wing sweep is a very important parameter since for large wing sweep angles, bending modes of the wing provide camber-like distortions along the wing chordlines thereby effecting changes in downwash and the unsteady aerodynamic loads essential to incite the flutter instability. It was desirable to vary vertical spacing between the wing and horizontal tail, but this was not readily practical for the model design selected. Most tests were therefore conducted with the wing and tail in the same plane. However, a limited series of tests were performed with the tail plane rotated to provide 45° of dihedral relative to the tail plane.

A summary of some of the model flutter data is given in Fig. 5. The flutter velocity is plotted against wing sweep for various ratios between cantilever wing bending and fuselage

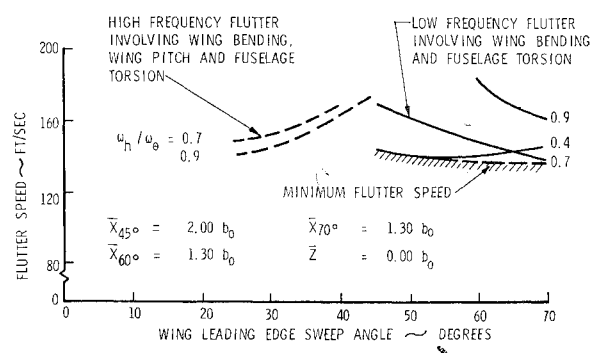


Fig. 5 Experimental variations of model flutter speed with wing sweep angle.

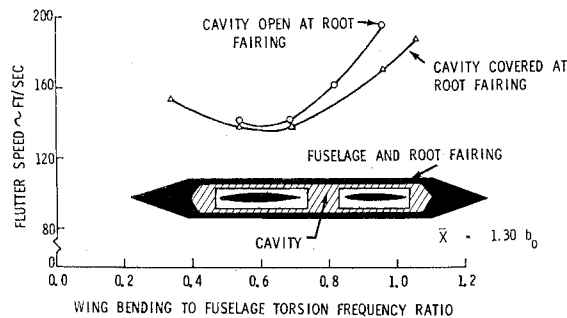


Fig. 6 Fuselage cavity effects on flutter speeds, 70° wing sweep (experimental data)

torsion frequencies. The dashed lines for frequency ratios of 0.7 and 0.9 at low-sweep angles represent trends of a higher frequency (11.0 Hz) flutter mode involving wing pitch, due to flexibilities near the pivot and its support, as well as wing bending and fuselage torsion motions. The coupled pitching mode is near 14 Hz at zero airspeed. The solid lines for frequency ratios of 0.9, 0.4 and 0.7 represent trends of the lower frequency mode (6–9 Hz), involving primarily wing bending and fuselage torsion. This is the more critical mode which causes lower flutter speeds for the higher wing sweep angles. This flutter mode occurs between the first two zero airspeed elastic modes just described. These subsonic model tests show that the trend of the low-frequency flutter mode with wing sweep is a function of frequency ratio or tuning. For the higher frequency ratios (0.7–0.9), the trends are generally quite similar to those reported by Topp et al.,¹⁷ as shown in Fig. 1. For low-frequency ratios, there is very little variation of flutter speed for high-wing sweep angles. The shaded line shows the envelope of lowest flutter speeds obtained by varying the frequency ratio at each sweep angle. The “critical frequency ratio” for minimum flutter velocity varies from 0.3 for 45° wing sweep to slightly above 0.6 for 70° wing sweep. Stated in other words, for high-wing sweep angles, minimum flutter speeds occur if the first antisymmetric wing bending frequency (model free to roll but fuselage rigid) is slightly lower (0.9 times) than the fuselage torsion frequency (fuselage free but wing and tail rigid).

Initial model tests were conducted with an open cavity in the root fairing to facilitate model parameter changes. Tufts were placed over the aft fuselage and horizontal tail. The behavior of the tufts indicated poor flow over the tail with the cavity open. Tests were conducted to determine the effect of this open cavity. Results are shown in Fig. 6. There is a 4% increase in velocity at a frequency ratio of 0.68 and a 12% increase at a frequency ratio of 0.97. Thus, it is essential in some cases to simulate the airplane cavity condition in model tests. The remaining tests were therefore conducted with the cavity filled with plugs and all data presented herein are for the filled cavity.

Theoretical Results and Comparison with Test Data

Flutter analyses were conducted using the roll mode and four flexible natural modes of vibration. Oscillatory aerodynamic loads were initially predicted by the first generation doublet lattice method¹⁵ which accounted for the aerodynamic interference effects between coplanar wing and tail. Some check calculations were conducted²³ using the kernel function method¹⁵ to predict the airloads. Results were essentially identical to the doublet lattice method data.

Some theoretical results are given in Fig. 7 for a wing sweep of 60°. When 100% (0% reduction) of the oscillatory airloads are acting on the tail due to both wing and tail motions, flutter occurs in the low-frequency wing bending-

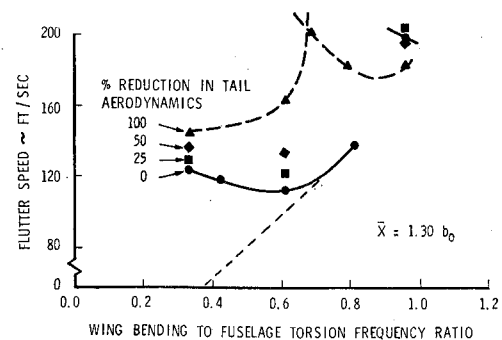


Fig. 7 Effect of tail aerodynamics on calculated flutter speeds, 60° wing sweep.

fuselage torsion flutter mode. Minimum flutter speeds are obtained near a frequency ratio of 0.6 due to the tuning mechanism previously mentioned. Arbitrary reductions were made in total aerodynamic loads on the tail induced by both wing and tail motions. The flutter speed in the low-frequency mode increased proving that airloads on the tail are detrimental. However, this flutter phenomenon can occur in the complete absence of all tail aerodynamic loads (100% reduction) thereby indicating that the prime coupling or instability tendency rests in wing and fuselage parameters for this configuration. The ratio of minimum flutter speeds for the condition with full aerodynamic loads on the tail to the condition with no aerodynamic loads on the tail is 0.80. Another feature which is noticeable is the tendency for the flutter speed to be proportional to frequency ratio for a small frequency ratio range just above the minimum velocity region for full aerodynamic load. The higher frequency flutter mode is evident in the flutter predictions for frequency ratios above 0.7. Some of the flutter model strain gage data indicated response in this higher frequency mode and the imminence of this flutter. Another interesting result from analyses (Fig. 8) was that an inch shorter wing semispan yielded calculated flutter speeds which were 3% and 10% lower than the flutter speeds of the longer wing for frequency ratios 0.62 and 0.82, respectively.

Flutter model data obtained for the 60° swept back wing and the coplanar tail for two different longitudinal separations are shown in Fig. 9, together with corresponding calculated results. The analyses predict the flutter velocity trends very well and indicate little difference in trends for these two longitudinal separations. The theory is about 18% conservative at minimum velocities near a frequency ratio of 0.5–0.6. For higher frequency ratios, theory shows a more rapid increase in flutter speed than shown by test data, particularly for the lower longitudinal separation. The conservative predictions of theory for minimum velocities may be due to thickness and viscous effects. The wing is likely blocking the

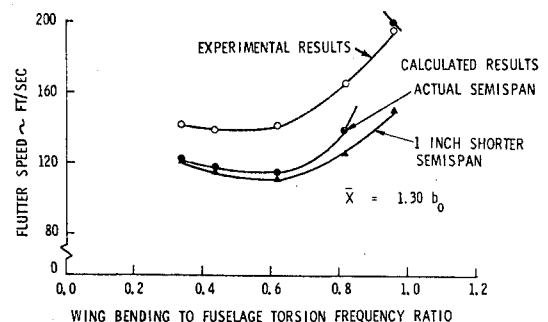


Fig. 8 Effects of wing semispan on calculated flutter speeds, 60° wing sweep.

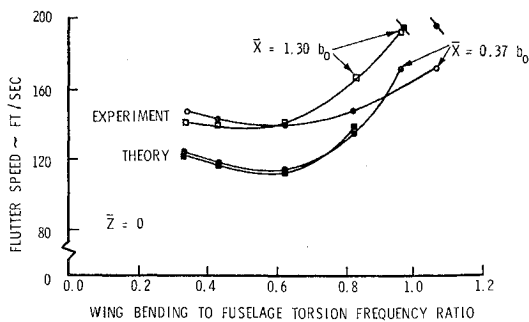


Fig. 9 Comparison of experimental and calculated flutter speeds, 60° wing sweep.

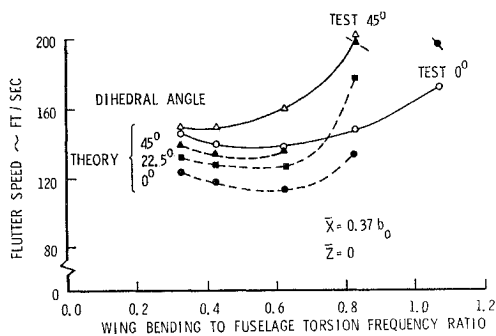


Fig. 10 Comparison of experimental and calculated flutter speeds for various tail dihedral angles, 60° wing sweep.

tail flow. This explanation seems to be a good possibility since tuft behavior indicated that flow over the tail was less than ideal even after the wing root-fuselage fairing cavities were plugged.

The effects of horizontal tail dihedral are shown in Fig. 10. Both test and theoretical data show that tail dihedral is beneficial. It is to be noted that the calculated results are based on the assumption that the mechanical properties of the wing-tail-fuselage mechanism remain unchanged as variations in longitudinal and vertical separation and dihedral angles are made. Thus, only aerodynamic effects are determined. The tail is moved out of the strongest influence of the oscillating wing wake thereby reducing wing interference loads on the tail and their detrimental influences. Test data indicate a 13% increase in flutter speed when the tail dihedral is changed from 0° to 45° near a frequency ratio of 0.6. The second generation doublet lattice method¹⁶ was used in the analyses and predicts a slightly higher change of 21% for the

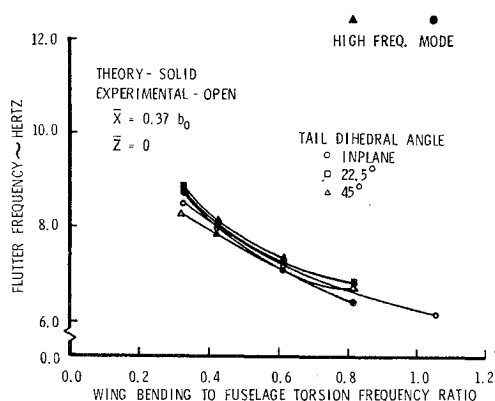


Fig. 11 Comparison of experimental and calculated flutter frequencies for various tail dihedral angles, 60° wing sweep.

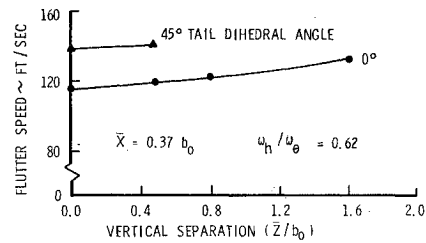


Fig. 12 Effect of vertical separation on flutter speed, 60° wing sweep (analytical results).

same frequency ratio. The general trend of flutter velocity with frequency ratio for 45° of tail dihedral is predicted. Theory indicates larger incremental increases in flutter speed due to dihedral changes at higher frequency ratios (0.82). Predicted flutter frequencies (Fig. 11) and their variations with tail dihedral and wing bending to fuselage torsion frequency ratio agree very well with available test data. The variation of predicted flutter frequency with tail dihedral for a given wing bending to fuselage torsion frequency ratio was very small.

Theoretical calculations were also made for several conditions where the tail plane was displaced parallel to the wing plane. The results, again obtained by the second generation doublet lattice method, are shown in Fig. 12. For the configuration where the horizontal tail has been displaced from 0% to 160% of the wing reference semichord, an increase of 16% in flutter velocity results. The variation of predicted flutter frequency with vertical displacement is small.

The computed flutter speed for the configuration where wing and tail centerlines are in the same plane, but the tail has 45° dihedral relative to the wing, is 21% higher than the coplanar flutter speeds. Approximately equal changes should be expected between these configurations since the outer region of the tail has been displaced about the same amount relative to the wing wake.

Analytical calculations were also made for the case where the horizontal tail was displaced parallel to the wing and the tail dihedral angle was varied from negative to positive angles thereby moving the tip of the tail from the vicinity of the strong portion of the wing wake to well out of it. Results shown in Fig. 13 show an increase of 22% in flutter velocity when the dihedral angle is changed from -12.5° to 45° for a frequency ratio of 0.62.

Transonic Tests and Correlations

To provide information on wing-fuselage-horizontal tail flutter at high speeds, the AFFDL defined a transonic flutter model program which was successfully conducted by Balcerak et al. of Cornell Aeronautical Laboratory in 1966 (Ref. 20). The wing and tail planforms were similar and of constant chord. Two wing-tail sweep angles, 45° and 60°, were investigated. Analyses for some of the test conditions were

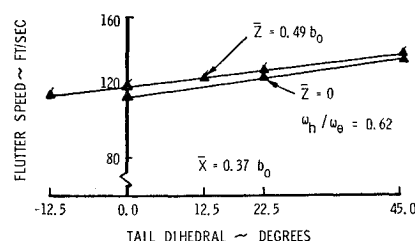


Fig. 13 Effects of vertical separation and tail dihedral angle on flutter speed, 60° wing sweep (analytical results).

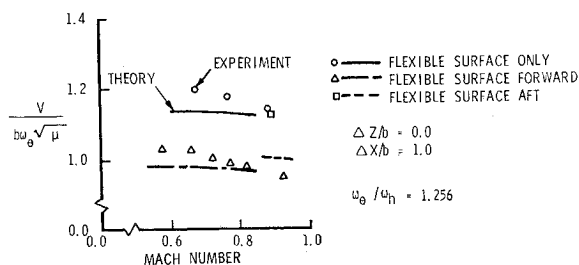


Fig. 14 Cornell transonic wing-tail flutter model results, 45° wing and tail sweep.

made by Albano et al.,¹⁵ using a nonplanar kernel function unsteady aerodynamic method. This development was based on extensions of methods defined by Laschka and Schmid¹¹ of Germany.

Figure 14 presents some exceedingly interesting data for a coplanar case. A rather ingenious approach was used by Cornell Aeronautical Laboratory. For one series of tests the more rigid surface was rotated out of the airstream so there was no aerodynamic interference but the mechanical coupling was present. For this test, only the more flexible surface was exposed to the airstream. For the other two conditions, both surfaces were in the airstream, but their positions were interchanged. The configuration with only the flexible surface exposed produces the highest flutter speeds. Notice again that this flutter is possible without wing-tail aerodynamic interference. Kernel function theory predicts the correct trends from 0.6 to 0.85 Mach number and is about 5% conservative. Intermediate flutter speeds are produced when the more rigid surface is forward (wing) and the more flexible surface is aft (tail). Kernel function theory is about 10% conservative for this configuration. The lowest flutter speeds are produced when the flexible surface is in the wing position and the more rigid surface is in the aft tail position. The flutter speeds are almost 20% lower than the condition with flexible surface only exposed. Kernel function results predict the trend with Mach number suprisingly well.

It should be noticed that the flutter velocity near a Mach number of 1.0 is decreasing so that the phenomenon will extend into the supersonic speed range. Thus, development of methods to predict unsteady aerodynamic loads for interfering surfaces is required for both transonic and low-supersonic speed regions. Li et al.²⁶ of the Boeing Company are now developing a Mach box method for the supersonic region for the AFFDL. The methods developed will be applied to the Cornell flutter models to estimate supersonic trends.

AGARD Wing-Horizontal Tail Configuration

The NATO Advisory Group for Aerospace Research and Development has selected standard configurations and parameters to make comparisons among various unsteady aerodynamic load prediction methods. Figure 15 shows the wing-horizontal tail configuration and the four antisymmetric modes selected. The spanwise variation of local lifts and moments due to these modes were calculated by AFFDL for both wing and tail for a Mach number of 0.8 and a reduced frequency of 1.5 based on wing semispan using the second generation doublet lattice method.¹⁶ All data computed are not shown since variations of the different interference loadings over the tail span are broadly similar.

Figure 16 shows the local lifts over the tail for the wing bending mode when the tail is displaced vertically 25% of the wing semispan (0.25Δ) and the dihedral is varied. The loading is increased and shifted outboard on the tail when dihedral

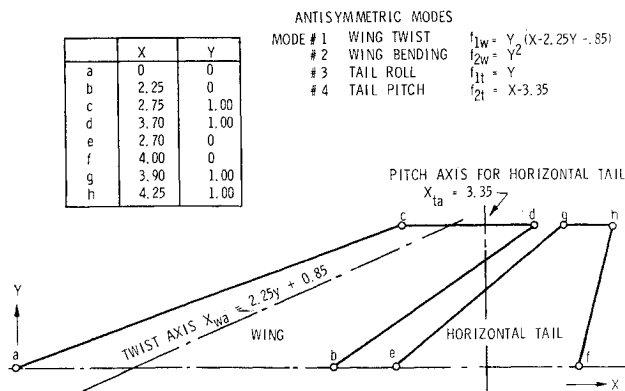


Fig. 15 AGARD wing-horizontal tail configuration.

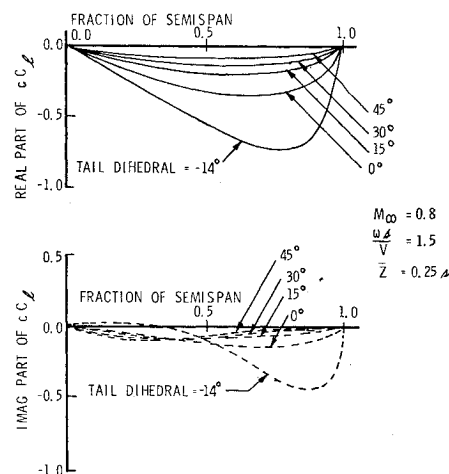


Fig. 16 Spanwise distribution of cC_l on the tail due to wing bending.

places the tail tip closer to the wing wake. Large reductions occur for all wing-induced tail loads as the tail is moved away from the strong wing wake. The magnitudes and the distributions of both the local lifts and moments over the wing change very slightly with the tail position and dihedral.

Figures 17 and 18 show the maximum moduli of the local tail lifts and moments for the wing bending vibration mode. The maximum tail local lift parameters decrease 81% when the tail dihedral is changed to 45° from the coplanar tail position. They increase 120% when tail dihedral changes from 0° to -14° for a configuration with 0.25Δ vertical displacement

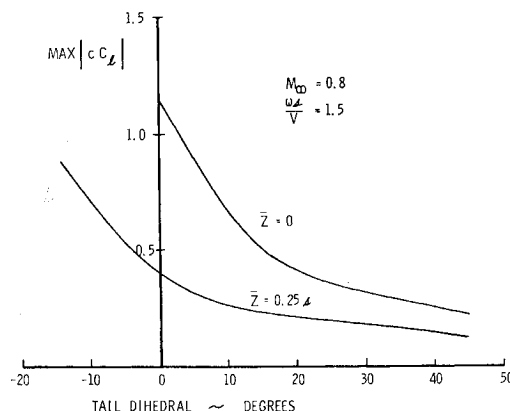


Fig. 17 Maximum $|cC_l|$ on the tail due to wing bending.

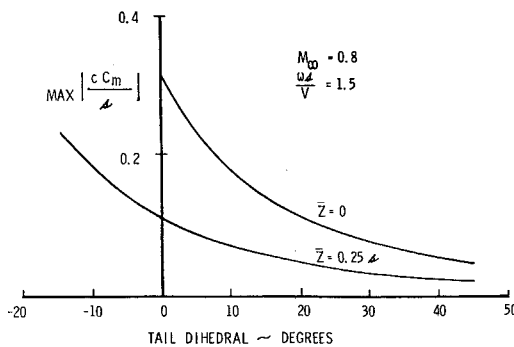


Fig. 18 Maximum $|cC_m/\delta|$ on the tail due to wing bending.

between the wing and tail. The reduction in the maximum local moment is 75% when the dihedral is changed from 0° to 45° (coplanar case) and the increase is 109% when the tail is displaced vertically 0.25δ and dihedral is changed to -14° from 0° . Similar results were obtained for the wing twist mode.

Figure 19 shows the variation of the magnitude of the generalized force coefficients for the tail modes due to unsteady aerodynamic pressure induced on the tail by the wing bending mode. A vertical displacement of 0.25δ reduces all the generalized forces by more than 50% for zero dihedral angle. Also, a positive dihedral angle change from 0° to 15° for 0.25δ displacement reduces the coefficients by approximately 50%. Negative dihedral (-14°) with 0.25δ positive vertical displacement causes approximately a doubling of the zero dihedral angle, generalized force coefficient. Again similar results were obtained for the wing twist mode.

The above percentage changes would not necessarily be reflected directly in flutter velocity changes since the wing aerodynamic loads contribute in large part to the instability as demonstrated by the analyses for the AFFDL flutter model and for the transonic Cornell flutter model discussed previously.

Closing Remarks

In summary, wing-fuselage-tail interacting flutter can cause low-flutter speeds and can be a critical design factor. Both mechanical-tuning and aerodynamic-interference couplings are important considerations. A valuable body of analytical and flutter model test information now exists for predicting and preventing this phenomenon. There are, however, several urgent needs. One is the development of

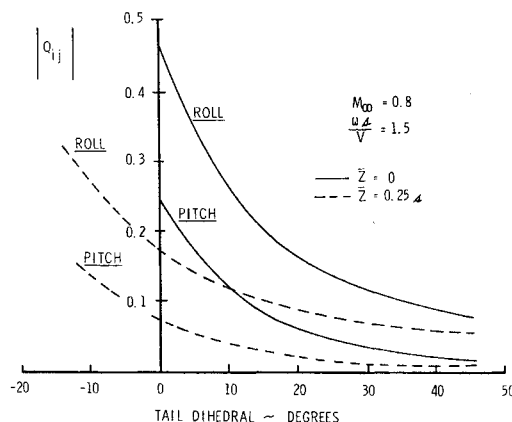


Fig. 19 Tail generalized force coefficient induced by wing bending vs tail dihedral.

reliable nonlinear transonic-low-supersonic unsteady aerodynamic load prediction methods. These are required for all configurations including isolated surfaces. Unsteady aerodynamic pressure measurements are also required to evaluate the theories and provide empirical corrections when analytical methods are inadequate. Exploratory supersonic analyses need to be completed to define an optimum supersonic flutter model program. This flutter model program should then be conducted to evaluate trends in the low-supersonic speed region, since test data indicate a decrease in flutter velocities beyond a Mach number of 1.0. These tests will also provide data to evaluate accuracies of supersonic unsteady aerodynamic load prediction methods. There is also a need to investigate the theoretical assumptions used for closely spaced wing and horizontal tails and determine proper flow conditions for the wing trailing edge and for the tail. Finally, methods are needed to account for the actual location and characteristics of the wing wake when determining their effects on tail flow and tail loading for practical lifting and maneuvering flight conditions.

References

- 1 Etkin, B., *Dynamics of Flight—Stability and Control*, Wiley, New York, 1959.
- 2 Ferrari, C., "Interaction Problems," *High Speed Aerodynamic and Jet Propulsion*, Vol. VII, Sec. C, Princeton University Press, Princeton, N. Y. 1957.
- 3 Stark, V. J. E., "Aerodynamic Forces on a Combination of a Wing and a Fin Oscillating in Subsonic Flow," TN 54, Feb. 1964, Svenska Aeroplan Aktiebolaget, Linköping, Sweden.
- 4 Davies, D. E., "Generalised Aerodynamic Forces on a T-Tail Oscillating Harmonically in Subsonic Flow," Rept. Structures 295, May 1964, Royal Aircraft Establishment, London, England.
- 5 Ashley, H., "Supersonic Airloads on Interfering Lifting Surfaces by Aerodynamic Influence Coefficient Theory," D2-22067, Nov. 1962, Boeing Co., Seattle, Wash.
- 6 Ashley, H., "Linearized Time Dependent Loading on Intersecting Lifting Surfaces," SID 63-1020, Aug. 1963, North American Aviation Inc., Downey, Calif.
- 7 Ashley, H., "Some Recent Developments in Interference Theory for Aeronautical Applications," MIT Fluid Dynamics Research Lab. Rept. 63-3, July 1963, MIT, Cambridge, Mass.; also *Proceedings of the Sixth Symposium of the Division of Fluid Mechanics*, Polish Academy of Science, Zakopane, Poland, Sept. 1963.
- 8 Laschka, B., "Zur Theorie der harmonisch schwingenden tragenden Fläche bei Unterschallanströmung," *Zeitschrift für Flugwissenschaften*, Vol. 11, No. 7, July 1963, pp. 265-292.
- 9 Ashley, H., Widnall, S., and Landahl, M. T., "New Directions in Lifting Surface Theory," *AIAA Journal*, Vol. 3, No. 1, Jan. 1965, pp. 3-16.
- 10 Landahl, M. T. and Stark, V. J. E., "Numerical Lifting Surface Theory—Problems and Progress," *AIAA Journal*, Vol. 6, No. 11, Nov. 1968, pp. 2049-2060.
- 11 Laschka, B. and Schmid, H., "Unsteady Aerodynamic Forces on Coplanar Lifting Surfaces in Subsonic Flow (Wing-Horizontal Tail Interference)," presented at AGARD Structures and Materials Panel Meeting, Sept. 25-29, 1967, Ottawa, Canada.
- 12 Laschka, B., "Interfering Lifting Surfaces in Subsonic Flow," presented at 29th AGARD Structures and Materials Panel Meeting, Sept.-Oct. 1969, Istanbul, Turkey.
- 13 Albano, E. and Rodden, W. P., "A Doublet Lattice Method for Calculating Lift Distributions on Oscillating Surfaces in Subsonic Flows," *AIAA Journal*, Vol. 7, No. 2, Feb. 1969, pp. 279-285.
- 14 Kalman, T., Rodden, W., and Giesing, J., "Application of the Doublet-Lattice Method to Nonplanar Configurations in Subsonic Flow," *Journal of Aircraft*, Vol. 8, No. 6, June 1971, pp. 406-413.
- 15 Albano, E., Perkinson, F., and Rodden, W., "Subsonic Lifting Surface Theory Aerodynamics and Flutter Analysis of Interfering Wing/Horizontal Tail Configurations," AFFDL-TR-70-59, Sept. 1970, Air Force Flight Dynamics Lab., Wright-Patterson Air Force Base, Ohio.
- 16 Giesing, J., Kalman, T., and Rodden, W., "Subsonic Unsteady Aerodynamics for Wing-Fuselage and Wing-Pylon-Store Combinations," AFFDL-TR-71-5, to be published by Air Force Flight Dynamics Lab., Wright-Patterson Air Force Base, Ohio.

¹⁷ Topp, L. J., Rowe, W. S., and Shattuck, A. W., "Aeroelastic Considerations in the Design of Variable Sweep Airplanes," ICAS Paper 66-12, Sept. 1966, Fifth International Congress of the Aeronautical Sciences, London, England.

¹⁸ Sensberg, O. and Laschka, B., "Flutter Induced by Aerodynamic Interference Between Wing and Tail," *Journal of Aircraft*, Vol. 7, No. 4, July-Aug. 1970, pp. 319-324.

¹⁹ Shelton, J. D., Tucker, P. B., and Davis, J. C., "Wing-Tail Interaction Flutter of Moderately Spaced Tandem Airfoils," AIAA Paper 69-57, New York, 1969.

²⁰ Balcerak, J. C., "Flutter Tests of Variable Sweep Configurations," AFFDL-TR-68-101, Sept. 1968, Air Force Flight Dynamics Lab., Wright-Patterson Air Force Base, Ohio.

²¹ Triplett, W. E., Burkhart, T. H., and Birchfield, E. B., "A Comparison of Methods for the Analysis of Wing-Tail Interaction Flutter," *Journal of Aircraft*, Vol. 8, No. 5, May 1971, pp. 361-367.

²² *Proceedings of the Symposium on Unsteady Aerodynamics for*

Aeroelastic Analyses of Interfering Surfaces, AGARD-CP-80-71, Nov. 1970, Tonsberg, Norway.

²³ Mykytow, W. J., Noll, T. E., Huttzell, L. J., and Shirk, M. H., "Subsonic Flutter Characteristics of a Variable Sweep Wing and Horizontal Tail Combination," AFFDL-TR-69-59, Nov. 1970, Air Force Flight Dynamics Lab., Wright-Patterson Air Force Base, Ohio.

²⁴ Bisplinghoff, R. L., Ashley, H., and Halfman, R. L., *Aeroelasticity*, Addison-Wesley, Reading, Mass. 1955.

²⁵ Dugundji, J., "On the Calculations of Natural Modes of Free-Free Structures," *Journal of the Aerospace Sciences*, Vol. 28, No. 2, Feb. 1961, pp. 164-166.

²⁶ Li, J. M., Borland, C. J., and Hogley, J. R., "Prediction of Unsteady Aerodynamic Loadings on Nonplanar Wings and Wing-Tail Configurations in Supersonic Flow," to be published as AFFDL-TR, Air Force Flight Dynamics Lab., Wright-Patterson Air Force Base, Ohio.